TITLE PAGE

EX VIVO EXPANSION POTENTIAL OF MURINE HEMATOPOIETIC STEM CELLS: A RARE PROPERTY ONLY PARTIALLY PREDICTED BY PHENOTYPE

Qinyu Zhang[1], Anna Konturek-Ciesla[1], Ouyang Yuan[1], David Bryder[1]

[1]Division of Molecular Hematology, Department of Laboratory Medicine, Lund Stem Cell Center, Faculty of Medical, Lund University, 221 84 Lund, Sweden.

Corresponding author:
David Bryder, DMH, BMC B12, Lund University, 221 84 Lund, Sweden +46706423951, David.Bryder@med.lu.se

Running title: HSC expansion *in vitro*

Manuscript information:
Text word count: 3951
Abstract word count: 226
Number of tables: 1
Number of figures: 5
Number of references: 43

Key point:
Ex vivo self-renewal is an intrinsic property of rare candidate HSCs, with implications for assessments of HSC activity by transplantation.

ABSTRACT

Hematopoietic stem cells (HSCs) reside at the apex of hematopoiesis, can maintain this function for life, and are the functional units in clinical bone marrow transplantation. Limitations in HSC numbers not only restricts their clinical use but also several embodiments of experimental research. A highly defined *ex vivo* culture system was recently shown to support robust expansion of *in vivo* HSC activity, prompting us to explore this system further. Over a 3-week culture period, only 0.1% of cultured cells retained the original input HSC phenotype, but these cells contained virtually all functional long-term HSC activity. Despite a low frequency of candidate HSCs, the net functional HSC expansion was large and necessitated several adjustments to the classical competitive repopulation for quantification. The *ex vivo* differentiated progeny from candidate HSCs was rich in progenitor cell activity and allowed for radioprotection from even single cultured HSCs. Limited numbers of expanded HSCs allowed for long-term multilineage engraftment of unconditioned hosts, with expanded HSCs rapidly returning to quiescence in this *in vivo* setting. Finally, clonal barcoding and competitive repopulation experiments demonstrated that successful HSC expansion emanated from rare HSC clones that was only partially predicted by phenotype. While a culture system that robustly expands HSC activity have been a long-sought goal in experimental HSC biology, our studies highlight the large impact of cellular heterogeneity also for this aspect of HSC biology.

INTRODUCTION

Rare hematopoietic stem cells (HSCs) are the functional units in bone marrow transplantation (BMT) and gene therapy approaches via their ability for multilineage differentiation and long-term self-renewal[1]. However, restrictions in HSC numbers, the requirement of harsh host conditioning and challenges with how to genetically manipulate HSCs with retained function are barriers for BMT/gene therapy[2]. Without reliable models to appropriately assess human HSCs, the mouse remains a preferred model for experimental HSC biology, but also murine HSC biology associates with many of the aforementioned challenges.

Recently, culture conditions supporting efficient maintenance and expansion of murine HSCs were reported[3]. However, the expansion of functional *in vivo* HSC activity over a 28-day period (estimated to 236-899-fold) was not on par with the total cell expansion (>10^4-fold), demonstrating that large amounts of differentiated progeny were generated along with self-renewing HSC divisions[3]. Moreover, while HSCs might change some phenotypes in culture[4], candidate HSCs (cHSCs) by phenotype represented only a minor portion at the culture end-point[3]. While, *in vitro* differentiation complicates assessments of HSC expansion, it might also be beneficial. For instance, although HSCs can sustain hematopoiesis for life following BMT, they are poor in providing hematopoietic rescue from lethal host conditioning[5]. For this, progenitors that can rapidly supply the host with erythrocytes and platelets are needed[6,7].

When transplanted, *in vivo* HSC activity is typically determined using both quantitative and qualitative parameters[8], most commonly by comparing to a known amount of competitor cells[9]. However, although the competitive repopulation assay (CRA) represents a mainstay in experimental HSC biology, it associates with shortcomings often neglected. First, while clinical BMT aims at transplanting large numbers of HSCs[10,11], experimental murine BMT typically use limited HSC grafts, which can influence on HSC function[12]. Secondly, the CRA is from a quantitative perspective rather blunt, with sigmoidal rather than linear characteristics[9] and which limits the boundaries of the effects that can be measured. Thirdly, the CRA assesses HSC activity based on overall test cell chimerism, which might reflect poorly on the actual HSC activity[13]. At the same time, alternative assays such as limit dilution assays or single-cell transplantation assays are cumbersome, expensive and associated with ethical concerns. Newer developments in DNA barcoding have overcome some of these issues[14].

Another concern with BMT is the use of aggressive host conditioning to permit engraftment. While eradicating malignant cells is an important part of treatment regimens for leukemic patients, the fates of HSCs in conditioned hosts versus native hematopoietic contexts are dramatically different[15]. But transplantation into unconditioned recipients is inefficient and requires large amounts of transplanted HSCs to saturate available niches[16,17]. To achieve even limited HSC chimerism in unconditioned hosts can have strong long-term therapeutic effects[18] and many experimental approaches might benefit from avoiding host conditioning.

Here, apart from defining a set of parameters critical for *in vivo* assessment of HSC activity, we find that HSC heterogeneity was a key influencing factor for HSC expansion even among rigorously purified cHSCs. This determinism has broad implications not only for experiments involving *in vitro* manipulation of HSCs, but also when assessing normal HSC function by BMT.

MATERIALS AND METHODS

Mice

Adult (8-10-week-old) C57Bl/6N (CD45.2$^+$) female mice were purchased from Taconic. Transgenic Fgd5-ZsGreen-2A-CreERT2 mice[19] (JAX:027789) was a kind gift from Derrick Rossi. Mice were maintained in the animal facilities at BMC, Lund University, with procedures approved by a local ethical committee (permits M186-15 and 16468/2020).

BM transplantation

Mice used as recipients were 8-12 week-old. When conditioned, mice were lethally irradiated (950 cGy) >4h prior to transplantation. Conditioned mice received prophylactic ciprofloxacin (HEXAL, 125 mg/L in drinking water) for 2 weeks. Transplantations were performed by intravenous tail vein injection.

In vitro HSC culture

In vitro HSC cultures were performed using F12-PVA based culture condition as described[3]. In brief, 96-well flat-bottom plates (Thermo Scientific) were coated with 100 ng/ml fibronectin (Sigma) for >1 hour at 37 °C prior to sorting or splitting. HSCs were sorted into 200 µl HSC media (Supplementary Table 1) and expanded at 37°C with 5% CO_2 for up to 21 days. Media changes were performed 5 days after initiation of cultures and then every 2 days. For lentiviral library transduction pre-culture, the first media change was performed 24h after transduction and then as above. Cells were split at 1:2-1:4 when reaching 80-90% confluency. Details on transduction with barcode libraries and Cell Trace Violet (CTV) labelling is provided in the supplementary methods section.

Cell preparation

Mice were euthanized by cervical dislocation after which bones or spleens were extracted. Fetal cells were extracted from livers. Bones were crushed using a mortar and pestle and bone marrow (BM) cells were collected in ice-cold phosphate-buffered saline (PBS, Gibco) with 1% fetal bovine serum (Sigma-Aldrich) (FACS buffer), filtered (100 µm mesh) and washed. Fetal liver (FL) or spleen cells were brought into single cell suspension by grinding through a 100 µm mesh. BM or FL cells were cKit-enriched by anti-cKit-APCeFluor780 (eBioscience) staining and spleen cells were CD4-

enrihced by anti-CD4-APC-Cy7 staining, followed by incubation with anti-APC conjugated beads (Miltenyi Biotec). Magnetic separation was performed using LS columns (Miltenyi Biotec). cKit-enriched cells were washed and stained with fluorescently labeled antibodies for analysis or sorting. CD4-enriched spleen cells were washed and labeled with CTV.

Peripheral blood (PB) chimerism analysis after transplantation was done as previously described[20].

For analysis and/or sorting after *ex vivo* expansion, cultured cells were resuspended by pipetting and collected using FACS buffer. An aliquot was taken for cell counting using an Automated Cell Counter (TC20, BioRad).

Flow cytometry analysis and FACS sorting

Cells were kept on ice when possible, with the FACS buffer kept ice-cold. Staining, analysis and sorting were performed as previously described[12]. In brief, cells were resuspended in Fc-block (1:50, 5 x 10^6 cells/50 µl, InVivoMab) for 10 min and then for 20 min with a twice concentrated antibody staining mixture (Supplementary tables 2-9) at 4 °C in dark. In case biotinylated lineage markers were included, a secondary staining with streptavidin BV605 was performed for 20 min (1:400, 5 x 10^6 cells/100 µl, Sony) at 4 °C in dark. After a final wash, the cells were resuspended in FACS buffer containing propidium iodide (1:1000, Invitrogen).

All FACS experiments were performed at the Lund Stem Cell Center FACS Core Facility (Lund University) on Aria III and Fortessa X20 instruments (BD). Bulk populations were sorted using a 70-micron nozzle, 0.32.0 precision mask, and a flow rate of 2 - 3K events/s. HSCs for single cell culture were index sorted. FACS analysis was performed using FlowJo version 10.8.0 (Tree Star Inc.).

Statistical test

Statistical analyses were performed using Microsoft Excel and Graphpad Prism 9. Significance was calculated by Mann-Whitney tests. Statistical significances are described in figure legends for the relevant graphs. In all legends, n denotes biological replicates.

RESULTS

In vivo HSC activity is restricted to cells expressing high levels of EPCR

We first assessed the *in vivo* reconstituting activity of cHSCs with different phenotypes. The endothelial protein C receptor (EPCR or PROCR/CD201) is highly expressed on BM HSCs[21], while CD41 (ITGA2B) was suggested to be functionally relevant for HSC maintenance and homeostasis[22]. Based on expression of EPCR and CD41, we isolated 4 subfractions within $Lin^{-}Sca1^{+}cKit^{+}CD150^{+}CD48^{-/low}$ (SLAM LSK) cells (Fig 1A). 50 cells from each fraction were transplanted with 500,000 unfractionated BM (WBM) competitor cells (Fig 1B). The reconstitution from the three $EPCR^{high}$ fractions was restricted to the PB myeloid lineages 4-week post-transplantation (Fig 1C), while most of these recipients displayed robust long-term multilineage reconstitution accompanied by equivalent cHSC chimerism in the BM (Fig 1C-D). $EPCR^{high}CD41^{-}$ cells produced slightly more lymphoid cells than the $EPCR^{high}CD41^{+}$ cells at the end-point (Fig S1), but the cHSC chimerism in the BM was very similar (Fig 1D). In contrast to Gekas et al.[22], we failed to observe that staining with the MWreg30 clone compromises HSC engraftment. Transplantation of $EPCR^{-}$ cells failed to associate with either long-term PB or BM cHSC chimerism (Fig 1C-D).

Next, single SLAM LSKs co-stained for EPCR were index sorted and expanded 21 days *ex vivo* followed by transplantation into individual lethally irradiated mice. Mice receiving progeny from SLAM LSK EPCR higher cells were more efficiently radioprotected (Fig. 1E). Thereafter, we initiated cultures with 50 $EPCR^{+}$ SLAM LSK cells separated into $EPCR^{high}$ or $EPCR^{low}$ fractions. Mice transplanted with cells expanded from $EPCR^{high}$ cells radioprotected all 5 recipients, while 2 out of 5 animals receiving the progeny of $EPCR^{low}$ cells survived long-term. As expected, surviving mice displayed exclusive test-cell derived myelopoiesis long-term after transplantation (Fig. 1F).

Taken together, this established that HSC activity was restricted to $EPCR^{high}$ HSCs and such cells could effectively generate progeny *in vitro* that rescue mice from lethal irradiation. Therefore, we operationally defined cHSCs as $EPCR^{high}$ SLAM LSK.

Phenotypic heterogeneity from *ex vivo* expanded cHSCs

A PVA-dependent cell culture system was reported to efficiently support HSC activity *ex vivo* over several weeks[3]. To detail the phenotype of such cultures, we expanded

aliquots of 50 cHSCs *ex vivo* for 14-21 days, followed by multicolour phenotyping (Fig 2A). An average of 0.5 million (14 days) and 13.6 million cells (21 days) were generated from 50 cHSCs (Fig 2B). This associated with a phenotypic heterogeneity that increased over time (Fig 2C). Assuming HSCs retain their phenotype, we quantified EPCR^{high} SLAM LSKs and observed a decrease in frequency over time (Fig 2D). Numerically, this was counteracted by the overall proliferation in cultures. Thus, quantification of cHSCs translated into an average expansion of 54-fold (26- to 85-fold) and 291-fold (86- to 1,273-fold) at 14 and 21 days, respectively (Fig 2D). To explore if other markers could provide additional phenotypic information, we used an *Fgd5* reporter mouse model previously shown to mark HSCs[19]. After culture, all EPCR^{high} SLAM LSK cells were positive for Fgd5 (Fig 2E), meaning that Fgd5 expression provided little additional information over the cell surface markers used.

Collectively, these results demonstrated robust expansion of cHSCs using the PVA-based culture system, albeit with parallel generation also of many other cells.

Functional HSC activity can be prospectively associated to a minor Lin^{-}Sca^{+}cKit^{+}EPCR^{+}CD150^{+}CD48$^{-/low}$ fraction within *ex vivo* cultures

Next, we explored the possibility to prospectively isolate HSCs with *in vivo* long-term multilineage repopulating activity from cHSC cultures. 500 cHSCs were isolated and cultured *ex vivo* for 21 days. The expanded cells were separated into two equal portions: one portion was kept unfractionated, while three subpopulations of CD150^{+}LSKs: EPCR^{high}CD48$^{-/low}$, EPCR^{high}CD48^{+} and EPCR^{-} were sorted from the other portion. The fractions were transplanted into lethally irradiated mice, such that each recipient received fractions equivalent to the expansion from 50 cHSCs (EE50) together with 500,000 competitor WBM cells (Fig 3A).

Stable and very high long-term multilineage reconstitution was observed in all recipients of unfractionated cultured cells. By contrast, test-cell derived reconstitution was not recovered from EPCR^{-} cells (Fig 3B and Fig S2). EPCR^{high}CD48^{+} cells produced very high reconstitution levels short-term after transplantation, but the chimerism from these cells dropped considerably over time (Fig 3B and Fig S2). This differed strikingly from recipients receiving the minor fraction of EPCR^{high}CD48$^{-/low}$ cells, which presented with robust long-term multilineage reconstitution (Fig 3B and Fig S2). While almost no cHSC chimerism was observed in recipients of EPCR^{high}CD48^{+} cells,

some chimerism was observed for progenitors downstream of HSCs. By contrast, very high chimerism was observed for all evaluated progenitor fractions, including cHSCs, in recipients of EPCR^{high}CD48$^{-/low}$ cells (Fig 3C).

These data established that functional *in vivo* HSC activity following culture was, similar to BM HSCs, exclusively retained within the EPCR^{high}CD48$^{-/low}$ fraction. By contrast, only transient multilineage reconstitution was observed from EPCR^{high}CD48^{+} cells. Finally, EPCR^{-} cells was devoid of HSC activity, similar to that observed from such cells when unmanipulated (Fig 1).

Quantification of HSC activity in *ex vivo* expansion cultures

Expanded cHSCs presented with a vastly higher reconstitution activity compared to freshly isolated cHSCs, and mostly fell out of range for accurate quantification (Fig 3B). We therefore assessed the impact of lowering the amount of input cHSCs and enhancing the amount of competitor cells. Aliquots of 10 cHSCs were cultured and expanded for 21 days. Cells from each culture (EE10) were next mixed with 2 or 20 million (2M or 20M) competitor WBM cells followed by transplantation (Fig 4A, 'individual'). We also included a group in which EE50 cHSCs were mixed with 10 million WBM cells and split among 5 lethally irradiated recipients (Fig 4A, 'pooled').

Although robust reconstitution was observed in most recipients in the 'individual' groups (Table 1, Fig 4B-C, Fig S3A-B), levels of test-cell derived cells varied extensively among recipients. To quantify the HSC activity in each recipient, we calculated the repopulating units (RUs)[9] for each lineage and recipient separately at the experimental end-point (Table 1). Short-lived myeloid cells has been proposed as a better indicator of ongoing HSC activity[23], and in agreement with this, we observed a high correlation between the RU^{myeloid} and RUs for cHSCs in the BM (Table 1). We observed a much more consistent HSC activity in between recipients of 'pooled' cells (Table 1, Fig 4B-C), confirming that the differential chimerism in recipients of limited cHSC numbers relates to an unresolved cellular heterogeneity of input cHSCs. RUs per initial cHSC were calculated for freshly isolated BM cHSCs (the three EPCR^{high} groups from Fig 1B) and following 3-week culture ('pooled' group). This revealed 461- and 70-fold increases in PB myeloid and BM cHSC chimerism in recipients of *ex vivo* expanded cells, respectively, which is an estimate of the increase of functional HSC activity following *ex vivo* culture (Fig S3G).

Next, we assessed HSC clonality using a lentiviral barcoding approach[24]. Five aliquots of 1,000 cHSCs were transduced (35% infection rate) with a barcode library 48 hours after culture and then expanded for 19 days. Half of the expanded cells from each well were transplanted into one 'parental' recipient, respectively, while the other half was mixed with each other, with each 'daughter' recipient receiving 1/5 of the mixed cells (Fig 4D-i). 16-weeks post-transplantation, barcodes were extracted from BM myeloid cells as a proxy for the HSC activity. Following stringent filtering, we retrieved 223 unique barcodes in the 'parental' recipients, with a highly variable contribution (0.1% - 26.0%, Fig 4E-G). The same barcode in 'parental' and 'daughter' recipients demonstrates a shared clonal/HSC origin. Clones more robustly expanded should therefore have a higher chance of reconstituting more 'daughter' recipients, which was in agreement with our observations (Fig 4E). Such clones also associated with larger output in 'daughter' recipients (Fig 4F). We then assessed the clonal HSC activity following expansion. For this, cHSCs were *ex vivo* expanded for 13 days, provided with barcodes overnight, and transplanted into 4 lethally irradiated recipients (Fig 4D-ii). 16-weeks post-transplantation, we recovered 573 unique barcodes. The median clone sizes of HSCs post-culture were significantly smaller than the pre-culture clones (Fig 4G), which was expected as more clones (573 vs 223) were evaluated in the 'post-culture' setting. However, the frequency of dominantly contributing clones was significantly less abundant (Fig 4H), demonstrating a more even contribution from individual clones.

We also assessed how the PVA culture system support the *in vivo* activity of fetal liver (FL) cHSCs. 50 FL-cHSCs were sorted and cultured *ex vivo*. We observed an average 188-fold increase in cHSCs following 21-days culture (Fig S3D). To functionally evaluate *ex vivo* expanded FL-cHSCs, we used the 'pooled' approach and competed EE10 with either 2 or 20 million WBM cells (Fig S3C). *Ex vivo* expanded cells from FL-cHSCs contributed considerably to multilineage reconstitution (Fig S3E). However, compared to adult expanded cHSCs, we observed 5.7- and 6.6-fold lower reconstitution from FL-cHSCs within PB myeloid cells and cHSCs, respectively (Fig S3F-G).

Taken together, these experiments demonstrated robust increases in HSC activity following culture of cHSCs, albeit slightly less for FL-cHSCs. However, clonal barcode assessments revealed substantial variation in *ex vivo* expansion potential of even stringently purified cHSCs.

Ex vivo expanded cHSCs returns to a quiescent state following engraftment in unconditioned recipients

Successful engraftment in an unconditioned setting requires large numbers of HSCs/HSPCs[16], which reportedly can be accommodated by PVA-cultured HSCs[3]. To test this, we transplanted EE100 CD45.1$^+$ cHSCs into lethally irradiated or unconditioned CD45.2$^+$ recipients (Fig S4A). In lethally irradiated hosts, cultured cells reconstituted more than 90% of PB cells, with virtually exclusive contribution of donor cells to the myeloid lineages. By contrast, most of the unconditioned recipients lacked long-term reconstitution (Fig S4B). Given that CD45 mismatching might be a sufficient immunological barrier to prevent HSPC reconstitution[25], we instead transplanted expanded cells into unconditioned F1 CD45.1$^+$/CD45.2$^+$ hosts (Fig 5A). Clear long-term multilineage engraftment was observed in all these hosts (Fig 5B).

In the BM, cHSCs exist for the most part in a quiescent state, which contrasts the situation in cultures. To investigate to what extent *ex vivo* expanded cHSCs could return to quiescence following transplantation, we expanded 100 CD45.2$^+$ cHSCs for 21 days and stained all their progeny with CTV, prior to transplantation into CD45.1$^+$/CD45.2$^+$ hosts. As a control, we transplanted unmanipulated CD45.2$^+$ cKit-enriched BM cells (Fig 5C). Splenic CD4$^+$ enriched cells were co-transplanted as a control for non-dividing cells (Fig S4C). Reconstitution and cHSC fates were monitored biweekly for up to 8-weeks post-transplant. Although the phenotypic cHSC contribution in recipients receiving *ex vivo* expanded cells outnumbered the contribution from unmanipulated cells two-weeks post-transplantation, the levels became comparable later on (Fig 5D). Recipients from both groups showed high levels of CTV signal two-weeks post-transplantation, with the majority of donor EPCR$^+$ cHSCs having undergone fewer than 3 cell divisions. Over time, increasing numbers of cHSCs had proliferated within both groups and with similar patterns (Fig 5E-F), with a slightly higher number of undivided cHSCs retrieved from *ex vivo* expanded HSCs at all time points (Fig 5E). The most quiescent cHSCs associated with higher EPCR levels (Fig S4E), again attesting to the usefulness of EPCR to predict robust HSC activity.

Therefore, *ex vivo* expanded cHSCs can efficiently engraft immunologically matched hosts without conditioning. Under such conditions, expanded cHSCs can rapidly return to quiescence following transplantation.

DISCUSSION

Although many efforts have aimed to *in vitro* expand murine HSCs, the results have for the most part been disappointing[26]. A recent study suggested that the substitution of undefined serum products with the synthetic polymer PVA is one key determinant towards this goal[3]. Here, we detailed this culture system further.

While the PVA-system support HSC activity even from unfractionated BM cell preparations[27], the long-term repopulating HSCs (LT-HSCs) in cruder input cell preparations is very low. While having its own advantages, this makes it difficult to track the fates of cHSCs. Therefore, we consistently initiated cultures with more stringently purified cHSCs. As a starting point, we used cHSCs isolated based on a current standard SLAM phenotype ($Lin^{-}Sca^{+}cKit^{+}CD48^{-}CD150^{+}$)[28]. In agreement with previous reports[29], we observed that CD201/EPCR further enriches for LT-HSCs. This applied both to cHSCs isolated directly from the BM and following culture. Importantly, such cHSCs represented only a very minor fraction in cultures (0.6% and 0.1% of 2- and 3-week cultures, respectively) but contained all LT-HSC activity.

While our clonal barcoding experiments unequivocally demonstrated HSC self-renewal, the large spectra in expansion potential of individual cHSCs was noteworthy. This variation was reduced when assessing HSC activity following culture and aligns with the interpretation that the offspring of cHSCs that expand robustly in cultures exhibit less differences. Therefore, our data support the view that this (or other) culture systems might not support all types of LT-HSCs previously eluded to[30]. In a broader sense, this associates also with the general concept of “self-renewal” and that has recently been highlighted in studies on native hematopoiesis, where distinct but only slowly contributing LT-HSCs co-exist with more active progenitors that can also execute self-renewal divisions[12,31,32]. It appears that many aspects of this structure are re-created in cultures and, as we show, this requires as input the normally very slowly dividing and presumably most primitive LT-HSCs.

While the parallel self-renewal and differentiation in HSC cultures represent a fundamental difference compared to other *in vitro* stem cell self-renewal systems (e.g., for ES/iPS cells), where preferential self-renewal can be achieved, the differentiation of HSCs can be taken advantage of. We observed that even single cultured HSCs can enhance the speed of donor reconstitution and alleviate the effects of myeloablative conditioning, and the parallel self-renewal and differentiation can also be harnessed to approach HSC fate decisions at a molecular level[33]. However, as the expansion of

genuine LT-HSC activity is far from unlimited, a shortage of HSCs is by all likelihood still an obstacle for larger-scale screening efforts such as genome-wide CRISPR screens and larger small molecule screens.

We encountered several aspects of the CRA that are often neglected. First, the HSC activity when transplanted at limited numbers highlighted large variations in between recipients, which has been established previously in extensive single cell transplantation experiments[34-38]. While this concern has been raised previously[39], taking into account not only the repopulating activity but also clonal aspects has not reached wide use. Emerging barcoding technologies, by which a large number of clones can be evaluated in a single mouse, makes this easier. Secondly, the progeny from a relatively small number of cultured cHSCs (10-50 cells) vastly outcompeted "standard" doses of competitor cells, making quantification unreliable/impossible. This contrasted results from freshly isolated cHSCs transplanted at the same doses used to initiate cultures. While this concern could be overcome by adjusting the graft composition, extensive variation still existed among cultures that could be eliminated by using larger amounts of input cells and splitting the contents into individual recipients. This should have relevance also for normal HSC biology by highlighting intrinsic rather than stochastic regulation as the central determinant for persistent HSC function. A third consideration relates to the definition of ongoing HSC activity. We and others have previously established that this is best mirrored by the contribution to myelopoiesis[40,41]. When we assessed cultured EPCR^{+}CD48^{+} cells (with predominantly transient multilineage activity), we observed prominent long-term T cell contribution. Thus, short-lived non-self-renewing multipotent progenitors, which are generated in great numbers in culture, can contribute extensive (lymphoid) offspring in the long-term but should not be mistaken for ongoing HSC activity. This consideration is valid also for competitor grafts in the CRA (in the form of WBM cells), which contain numerous progenitor cells that can rapidly fill up a given (lymphoid) compartment. Thus, as opposed to the classic CRA, where the overall donor contribution is assessed[9], the contribution to short-lived lineages reflects better the ongoing HSC activity, with the contribution to lymphoid lineages serving as a qualitative parameter for multipotency.

Successful repopulation of non-conditioned hosts is based on the suggestion that large numbers of HSCs are needed to saturate those few BM niches available for engraftment[18,42]. Avoiding toxic myeloablation has apart from evident clinical

implications also a precedence in experimental murine HSC biology, where lethal myeloablation enforces vigorous HSC proliferation following transplantation[12], but which contrasts native contexts[12,31,32]. We observed that the CD45.1/CD45.2 differences are sufficiently immunogenic to mediate long-term graft failure in the non-conditioned setting, which in hindsight has been eluded to previously[18,25,43]. Thus, by matching hosts for CD45-isoforms, we could successfully obtain low-level (2-5%) long-term multilineage chimerism in adult non-myeloablated hosts from only 100 cHSCs. Intriguingly, despite being activated to proliferate *in vitro*, many cHSCs rapidly returned to a quiescent state *in vivo*, with the most dormant cHSCs exhibiting the most stringent HSC phenotype (EPCR^{high}SLAM LSKs). The possibility for non-conditioned transplantation should complement genetic lineage tracing models aimed at exploring both normal and malignant hematopoiesis in more native/physiological contexts[12,31,32].

In summary, although several aspects of the PVA system remain to be explored, a powerful *in vitro* self-renewal system has been a long-sought goal in HSC biology where HSCs have been notoriously difficult to uphold in an undifferentiated/self-renewal state. The merger of this system with recent advances in transplantation biology, genome engineering and single-cell techniques now holds promise for many exciting discoveries of relevance to both basic and more clinically-oriented hematopoietic research.

ACKNOWLEDGMENTS

We acknowledge Dr. Shabnam Kharazi for scientific discussions and technical support, Mr. Yun Sheng for advice on analysis for barcode sequencing and Prof. Hiromitsu Nakauchi and Dr. Adam C. Wilkinson for advice on cell cultures. The work was supported by grants from the Tobias Foundation, the Swedish Cancer Foundation and the Swedish Research Council to D.B. and the Royal Physiographic Society of Lund foundation to Q.Z and A.K-C.

AUTHORSHIP CONTRIBUTIONS

Q.Z. designed the research, performed experiments, analyzed data, and wrote the manuscript; A. K-C and O.Y. performed experiments and analyzed data; D.B. supervised the project, was responsible for funding acquisition, designed the research, analyzed data and wrote the manuscript.

CONFLICT OF INTEREST DISCLOSURES

The authors report no conflict of interest.

REFERENCES

1. Konturek-Ciesla A, Bryder D. Stem Cells, Hematopoiesis and Lineage Tracing: Transplantation-Centric Views and Beyond. *Frontiers in Cell and Developmental Biology*. 2022;10.
2. Walasek MA, van Os R, de Haan G. Hematopoietic stem cell expansion: challenges and opportunities. *Ann N Y Acad Sci*. 2012;1266:138-150.
3. Wilkinson AC, Ishida R, Kikuchi M, et al. Long-term ex vivo haematopoietic-stem-cell expansion allows nonconditioned transplantation. *Nature*. 2019.
4. Zhang CC, Lodish HF. Murine hematopoietic stem cells change their surface phenotype during ex vivo expansion. *Blood*. 2005;105(11):4314-4320.
5. Nakauchi H, Takano H, Ema H, Osawa M. Further characterization of CD34-low/negative mouse hematopoietic stem cells. *Ann N Y Acad Sci*. 1999;872:57-66; discussion 66-70.
6. Yang L, Bryder D, Adolfsson J, et al. Identification of Lin(-)Sca1(+)kit(+)CD34(+)Flt3- short-term hematopoietic stem cells capable of rapidly reconstituting and rescuing myeloablated transplant recipients. *Blood*. 2005;105(7):2717-2723.
7. Na Nakorn T, Traver D, Weissman IL, Akashi K. Myeloerythroid-restricted progenitors are sufficient to confer radioprotection and provide the majority of day 8 CFU-S. *J Clin Invest*. 2002;109(12):1579-1585.
8. Purton LE, Scadden DT. Limiting factors in murine hematopoietic stem cell assays. *Cell Stem Cell*. 2007;1(3):263-270.
9. Harrison DE, Jordan CT, Zhong RK, Astle CM. Primitive hemopoietic stem cells: direct assay of most productive populations by competitive repopulation with simple binomial, correlation and covariance calculations. *Exp Hematol*. 1993;21(2):206-219.
10. Barnett D, Janossy G, Lubenko A, Matutes E, Newland A, Reilly JT. Guideline for the flow cytometric enumeration of CD34+ haematopoietic stem cells. Prepared by the CD34+ haematopoietic stem cell working party. General Haematology Task Force of the British Committee for Standards in Haematology. *Clin Lab Haematol*. 1999;21(5):301-308.
11. Trebeden-Negre H, Rosenzwajg M, Tanguy ML, et al. Delayed recovery after autologous peripheral hematopoietic cell transplantation: potential effect of a high number of total nucleated cells in the graft. *Transfusion*. 2010;50(12):2649-2659.
12. Sawen P, Lang S, Mandal P, Rossi DJ, Soneji S, Bryder D. Mitotic History Reveals Distinct Stem Cell Populations and Their Contributions to Hematopoiesis. *Cell Rep*. 2016;14(12):2809-2818.
13. Bryder D, Sasaki Y, Borge OJ, Jacobsen SE. Deceptive multilineage reconstitution analysis of mice transplanted with hemopoietic stem cells, and implications for assessment of stem cell numbers and lineage potentials. *J Immunol*. 2004;172(3):1548-1552.
14. Lu R, Neff NF, Quake SR, Weissman IL. Tracking single hematopoietic stem cells in vivo using high-throughput sequencing in conjunction with viral genetic barcoding. *Nat Biotechnol*. 2011;29(10):928-933.

15. Busch K, Rodewald HR. Unperturbed vs. post-transplantation hematopoiesis: both in vivo but different. *Curr Opin Hematol*. 2016;23(4):295-303.
16. Brecher G, Ansell JD, Micklem HS, Tjio JH, Cronkite EP. Special proliferative sites are not needed for seeding and proliferation of transfused bone marrow cells in normal syngeneic mice. *Proc Natl Acad Sci U S A*. 1982;79(16):5085-5087.
17. Bhattacharya D, Czechowicz A, Ooi AG, Rossi DJ, Bryder D, Weissman IL. Niche recycling through division-independent egress of hematopoietic stem cells. *J Exp Med*. 2009;206(12):2837-2850.
18. Bhattacharya D, Rossi DJ, Bryder D, Weissman IL. Purified hematopoietic stem cell engraftment of rare niches corrects severe lymphoid deficiencies without host conditioning. *J Exp Med*. 2006;203(1):73-85.
19. Gazit R, Mandal PK, Ebina W, et al. Fgd5 identifies hematopoietic stem cells in the murine bone marrow. *J Exp Med*. 2014;211(7):1315-1331.
20. Sawen P, Eldeeb M, Erlandsson E, et al. Murine HSCs contribute actively to native hematopoiesis but with reduced differentiation capacity upon aging. *Elife*. 2018;7.
21. Balazs AB, Fabian AJ, Esmon CT, Mulligan RC. Endothelial protein C receptor (CD201) explicitly identifies hematopoietic stem cells in murine bone marrow. *Blood*. 2006;107(6):2317-2321.
22. Gekas C, Graf T. CD41 expression marks myeloid-biased adult hematopoietic stem cells and increases with age. *Blood*. 2013;121(22):4463-4472.
23. Domen J, Cheshier SH, Weissman IL. The role of apoptosis in the regulation of hematopoietic stem cells: Overexpression of Bcl-2 increases both their number and repopulation potential. *J Exp Med*. 2000;191(2):253-264.
24. Biddy BA, Kong W, Kamimoto K, et al. Single-cell mapping of lineage and identity in direct reprogramming. *Nature*. 2018;564(7735):219-224.
25. van Os R, Sheridan TM, Robinson S, Drukteinis D, Ferrara JL, Mauch PM. Immunogenicity of Ly5 (CD45)-antigens hampers long-term engraftment following minimal conditioning in a murine bone marrow transplantation model. *Stem Cells*. 2001;19(1):80-87.
26. Wilkinson AC, Igarashi KJ, Nakauchi H. Haematopoietic stem cell self-renewal in vivo and ex vivo. *Nat Rev Genet*. 2020;21(9):541-554.
27. Ochi K, Morita M, Wilkinson AC, Iwama A, Yamazaki S. Non-conditioned bone marrow chimeric mouse generation using culture-based enrichment of hematopoietic stem and progenitor cells. *Nat Commun*. 2021;12(1):3568.
28. Challen GA, Pietras EM, Wallscheid NC, Signer RAJ. Simplified murine multipotent progenitor isolation scheme: Establishing a consensus approach for multipotent progenitor identification. *Exp Hematol*. 2021;104:55-63.
29. Kent DG, Copley MR, Benz C, et al. Prospective isolation and molecular characterization of hematopoietic stem cells with durable self-renewal potential. *Blood*. 2009;113(25):6342-6350.
30. Haas S, Trumpp A, Milsom MD. Causes and Consequences of Hematopoietic Stem Cell Heterogeneity. *Cell Stem Cell*. 2018;22(5):627-638.

31. Sun J, Ramos A, Chapman B, et al. Clonal dynamics of native haematopoiesis. *Nature*. 2014;514(7522):322-327.
32. Busch K, Klapproth K, Barile M, et al. Fundamental properties of unperturbed haematopoiesis from stem cells in vivo. *Nature*. 2015;518(7540):542-546.
33. Weinreb C, Rodriguez-Fraticelli A, Camargo FD, Klein AM. Lineage tracing on transcriptional landscapes links state to fate during differentiation. *Science*. 2020;367(6479).
34. Yamamoto R, Wilkinson AC, Ooehara J, et al. Large-Scale Clonal Analysis Resolves Aging of the Mouse Hematopoietic Stem Cell Compartment. *Cell Stem Cell*. 2018;22(4):600-607 e604.
35. Yamamoto R, Morita Y, Ooehara J, et al. Clonal analysis unveils self-renewing lineage-restricted progenitors generated directly from hematopoietic stem cells. *Cell*. 2013;154(5):1112-1126.
36. Benz C, Copley MR, Kent DG, et al. Hematopoietic stem cell subtypes expand differentially during development and display distinct lymphopoietic programs. *Cell Stem Cell*. 2012;10(3):273-283.
37. Carrelha J, Meng Y, Kettyle LM, et al. Hierarchically related lineage-restricted fates of multipotent haematopoietic stem cells. *Nature*. 2018;554(7690):106-111.
38. Oguro H, Ding L, Morrison SJ. SLAM family markers resolve functionally distinct subpopulations of hematopoietic stem cells and multipotent progenitors. *Cell Stem Cell*. 2013;13(1):102-116.
39. Ema H, Nakauchi H. Expansion of hematopoietic stem cells in the developing liver of a mouse embryo. *Blood*. 2000;95(7):2284-2288.
40. Norddahl GL, Pronk CJ, Wahlestedt M, et al. Accumulating mitochondrial DNA mutations drive premature hematopoietic aging phenotypes distinct from physiological stem cell aging. *Cell Stem Cell*. 2011;8(5):499-510.
41. Domen J, Weissman IL. Hematopoietic stem cells and other hematopoietic cells show broad resistance to chemotherapeutic agents in vivo when overexpressing bcl-2. *Exp Hematol*. 2003;31(7):631-639.
42. Czechowicz A, Kraft D, Weissman IL, Bhattacharya D. Efficient transplantation via antibody-based clearance of hematopoietic stem cell niches. *Science*. 2007;318(5854):1296-1299.
43. Xu H, Exner BG, Chilton PM, Schanie C, Ildstad ST. CD45 congenic bone marrow transplantation: evidence for T cell-mediated immunity. *Stem Cells*. 2004;22(6):1039-1048.

TABLES

Table 1. RUs for each lineage in PB and for BM cHSCs of each recipient.

Recipients		*PB*	*B cells*	*T cells*	*Myeloid* cells	*BM cHSCs*
Individual BM EE10 + 2M	***#1***	6	6	6	4	12
	#2	31	35	19	27	75
	#3	21	23	17	35	70
	#4	98	144	46	57	21
	#5	1	1	2	0.03	0.4
Pooled BM EE10 + 2M	***#1***	101	78	173	583	49
	#2	110	84	120	516	82
	#3	87	68	103	248	130
	#4	101	70	149	384	187
	#5	65	127	186	331	112

** 1 RU equals to the reconstitution activity of 1 x10 ^{5} WBM cells.*

FIGURE LEGENDS

Figure 1. EPCR expression within the BM SLAM LSK fraction is a high-confidence predictor of transplantation-associated HSC activity

(A) Expression patterns of EPCR and CD41 within the BM LSK SLAM fraction. Gates depict the assessed cell fractions.

(B) Strategy used to assess the correlation of EPCR and CD41 expression to the *in vivo* HSC activity.

(C) Test-cell derived chimerism 4 and 16-weeks post-transplantation.

(D) Test-cell derived chimerism in BM EPCR^{+} SLAM LSKs.

(E) Correlation between duration of radioprotection and EPCR expression levels. BM LSK SLAM cells were co-stained with EPCR and index-sorted at one cell per well, cultured for 21 days, and the content of each well transplanted to individual recipients (n = 22). Correlation to mortality of individual mice was made by assessing which well was transplanted into which mouse and coupling this to the index-sorting information.

(F) Donor contribution in PB myeloid cells. Mice were transplanted with *ex vivo* expanded cells from either 50 SLAM LSK EPCR^{lower} (n = 5) or 50 SLAM LSK EPCR^{high} cells (n = 5) and assessments made 16 weeks after transplantation.

All data points depict values in individual recipients. Error bars denote SEM. The asterisks indicate significant differences. *, $p < 0.05$; **, $p < 0.01$. In E) a regression line was generated based on an end-point survival of 150 days (the time at which the experiment was terminated).

Figure 2. The phenotypic properties of HSC expansion cultures.

(A) Representative FACS plots of cHSCs cultured for 14 days. Cells with an EPCR^{high}CD48$^{low/-}$ phenotype represent phenotypic cHSCs.

(B) Overall cell expansion from 50 EPCR^{high} SLAM LSKs after 14- or 21-days of *ex vivo* culture.

(C) Frequency of cells expressing different stem cell markers in *ex vivo* cultures following 14 or 21 days of culture.

(D) Frequency and fold change of phenotypic cHSCs (EPCR^{high} SLAM LSKs) in *ex vivo* cultures after 14 or 21 days of culture.

(E) Representative FACS plots of cells expanded 14 days in *ex vivo* cultures using Fgd5-ZsGreen reporter cells. Mean values demonstrate the frequency of Fgd5^{+}Lin^{-}

Fcer1a$^-$ or Fgd5$^+$EPCR$^+$CD150$^+$Fcer1a$^-$LSK cells, respectively. Mean ± SEM value was calculated from 15 individual cultures initiated from 50 cHSCs.

All data points depict values from individual cultures initiated from 50 cHSCs. Error bars denote SEM. The asterisks indicate significant differences. **, $p < 0.01$; ***, $p < 0.001$; ****, $p < 0.0001$.

Figure 3. HSC activity can be prospectively isolated from cHSC cultures and associates to a minor EPCR$^+$ SLAM LSK fraction

(A) Strategy to assess the *in vivo* HSC activity of subfractions from *ex vivo* cultures.

(B) Test-cell derived chimerism in PB myeloid lineages over 24-weeks post-transplantation. Data represent mean values ± SEM (n = 5 for each group).

(C) Test-cell derived chimerism in BM progenitor subsets 24-weeks post-transplantation. Numbers indicate fold differences between the EPCR$^+$ CD48$^{-/low}$ and EPCR$^+$CD48$^+$ fractions, and data points depict chimerism levels in individual recipients.

Figure 4 Quantification of repopulating activity from expanded cHSCs

(A) Competitive transplantation strategies used to assess the repopulation of *ex vivo* expanded cHSCs.

(B) Test-cell derived PB reconstitution 16-weeks post-transplantation. Symbols denote individual mice and means ± SEM.

(C) BM cHSCs chimerism 16 weeks post transplantation. Symbols denote individual mice, and means ± SEM.

(D) Barcode approaches used to assess the clonal HSC contribution of *ex vivo* expanded HSCs before (i) or after (ii) *ex vivo* expansion.

(E) Clone sizes of unique barcodes in ‘parental’ recipients and their appearance in ‘daughter’ recipients, demonstrating extensive variation in expansion capacity among individual HSCs. Red lines indicate the median clone size in ‘parental’ recipients.

(F) Clone sizes of unique barcodes detected in BM myeloid cells of ‘parental’ recipients and their corresponding contribution in ‘daughter’ recipients. The red line denotes the correlation/linear regression.

(G) Clone sizes in ‘parental’ recipients transplanted with ‘pre-culture’ barcoded cells, or in recipients of ‘post-culture’ barcoded cells. Median clone sizes are shown with interquartile ranges.

(H) Frequency of barcodes and their clone sizes in recipients of pre- or post-cultured barcoded HSCs. BCs, barcodes.

All data points depict values in individual recipients or barcodes. Asterisks indicate significant differences. *, $p < 0.05$; ****, $p < 0.0001$.

Figure 5. Cultured cHSCs allow for transplantation into non-conditioned syngeneic recipients.

(A) Strategy to assess the ability of *ex vivo* expanded cHSCs to engraft unconditioned recipients. Symbols denote individual mice and means ± SEM.

(B) Test-cell derived PB reconstitution 24-weeks post-transplantation.

(C) Strategy used to assess the *in vivo* proliferation of *ex vivo* expanded cHSCs.

(D) BM cHSC chimerism 2-8 weeks post transplantation.

(E) Representative CTV label profiles of donor $EPCR^+$ cHSCs compared to negative control signal (host $EPCR^+$ cHSCs) and positive signal (donor $CD4^+$ spleen cells) at 2 or 8 weeks post-transplantation.

(F) Donor $EPCR^+$ cHSCs were evaluated for the number of cell divisions they had undergone through 8 weeks post-transplantation.

All data points depict values in individual recipients.

FIGURES

Figure 1, Zhang et al.

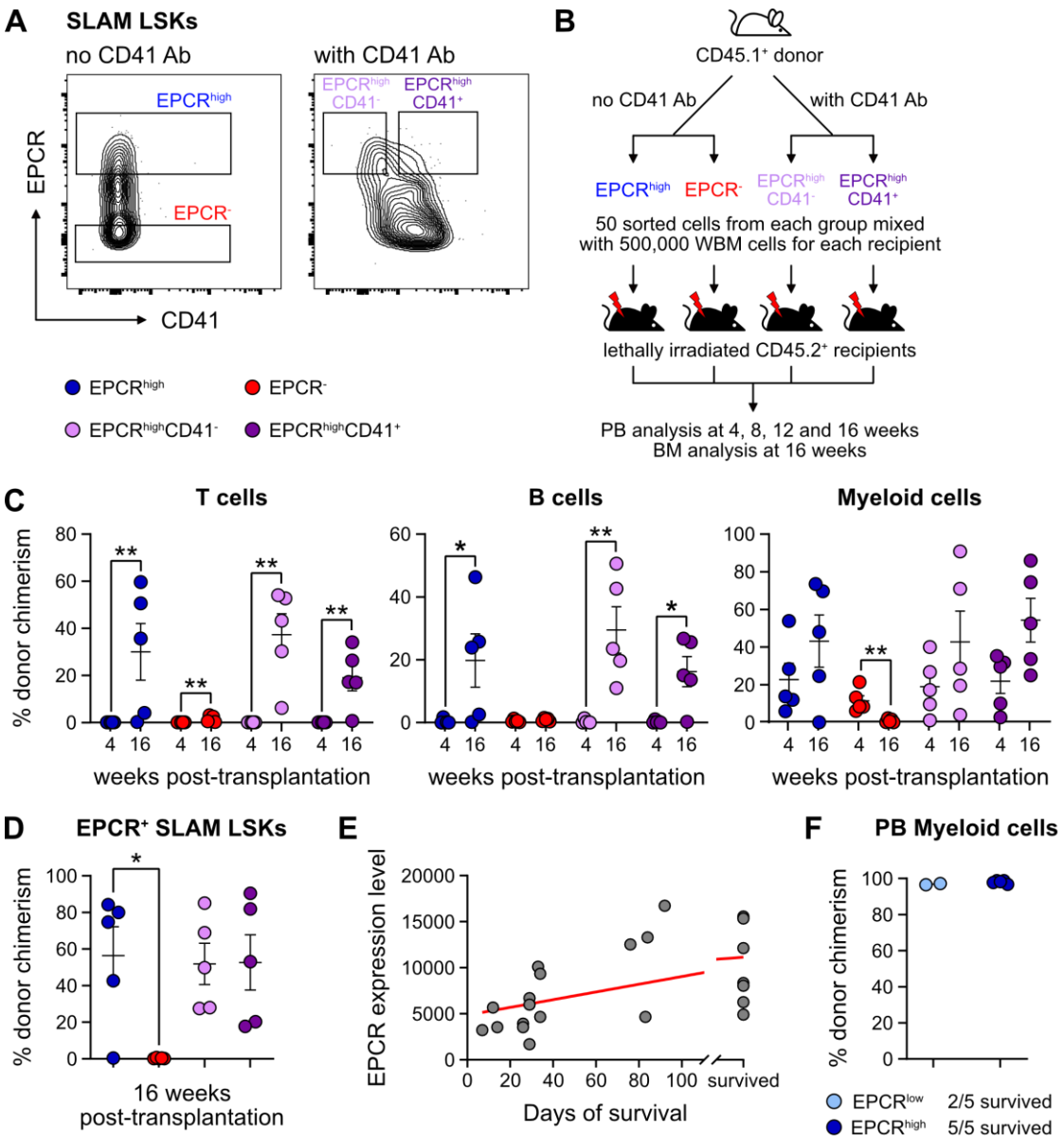

Figure 2, Zhang et al.

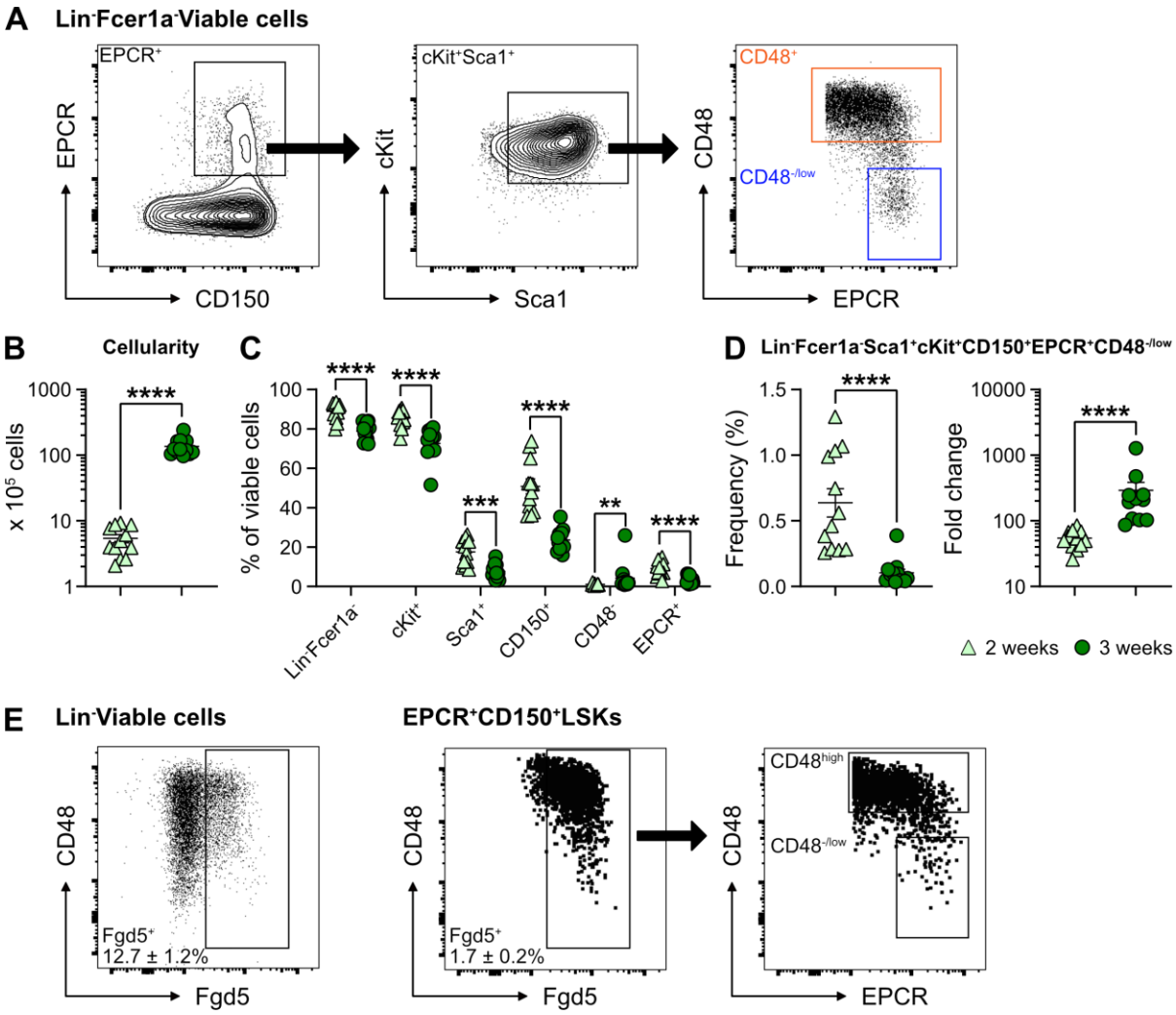

Figure 3, Zhang et al.

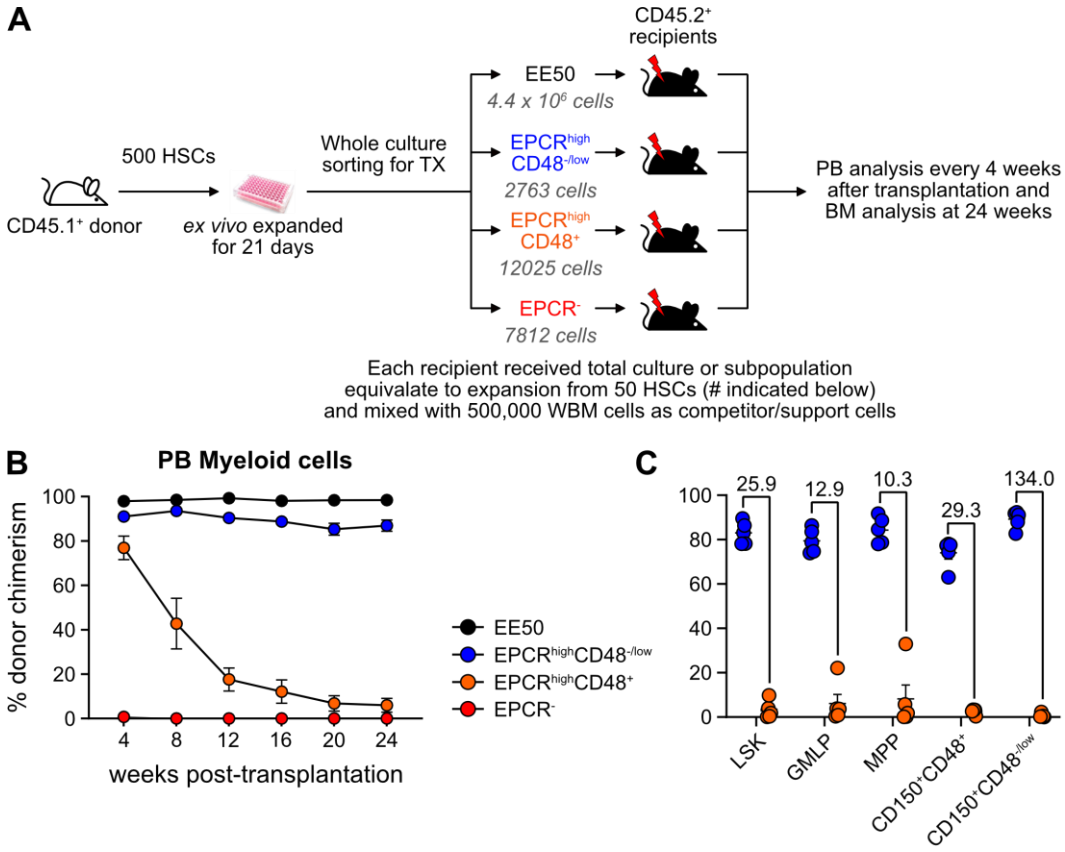

Figure 4, Zhang et al.

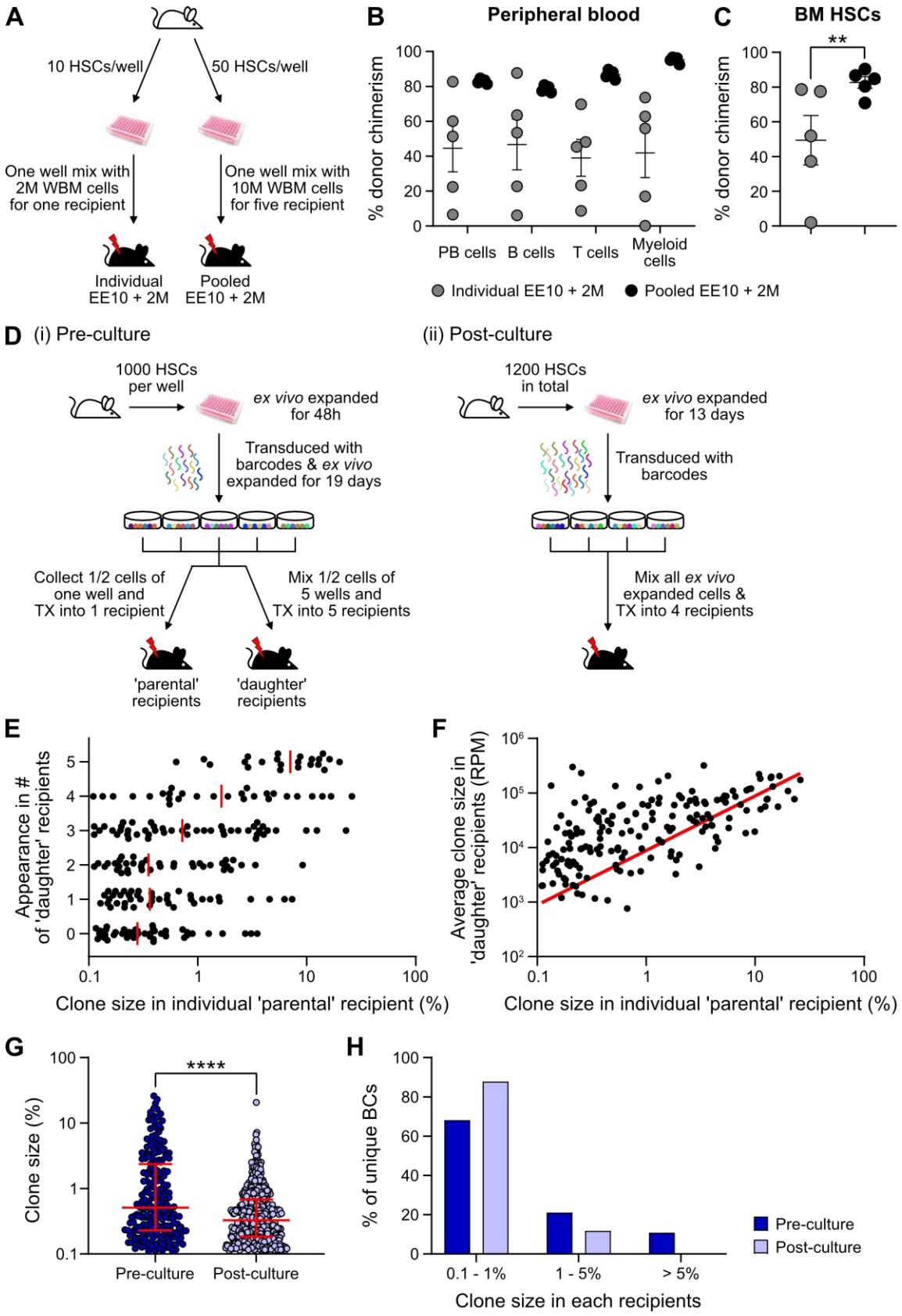
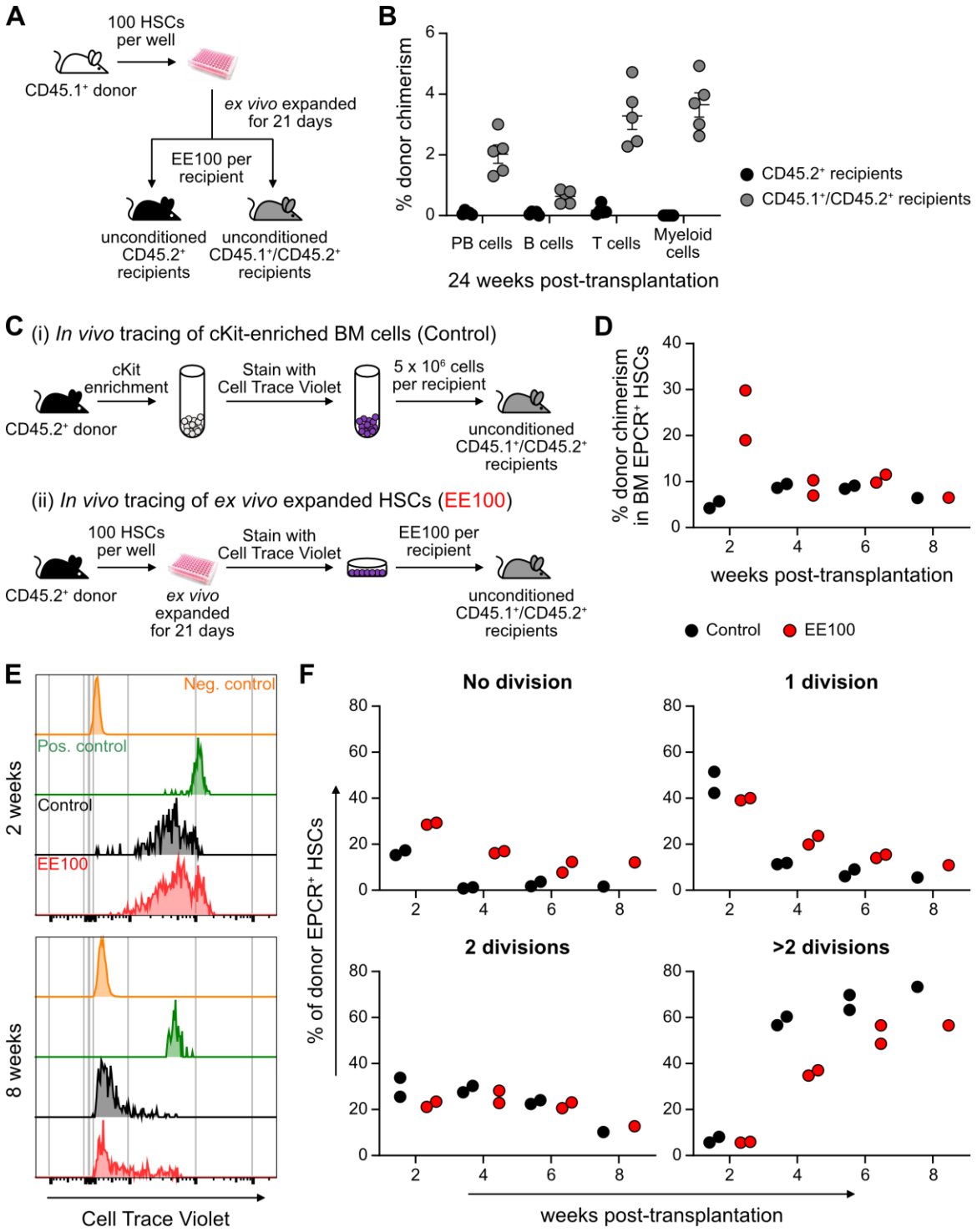
Figure 5, Zhang et al.